Original Article

GLYAT suppresses liver cancer and clear cell renal cell carcinoma progression by downregulating ROCK1 expression

Yechen Xia[1], Wentao Huang[2], Guang-Zhi Jin[1]^

[1]Hongqiao International Institute of Medicine, Tongren Hospital, Shanghai Jiao Tong University School of Medicine, Shanghai, China; [2]Department of Pathology, Tongren Hospital, Shanghai Jiao Tong University School of Medicine, Shanghai, China

Contributions: (I) Conception and design: GZ Jin, W Huang; (II) Administrative support: GZ Jin, W Huang; (III) Provision of study materials or patients: GZ Jin; (IV) Collection and assembly of data: Y Xia; (V) Data analysis and interpretation: Y Xia; (VI) Manuscript writing: All authors; (VII) Final approval of manuscript: All authors.

Correspondence to: Guang-Zhi Jin, PhD. Hongqiao International Institute of Medicine, Tongren Hospital, Shanghai Jiao Tong University School of Medicine, No. 1111 Xianxia Road, Shanghai 200336, China. Email: jgzhi@hotmail.com; Wentao Huang, PhD. Department of Pathology, Tongren Hospital, Shanghai Jiao Tong University School of Medicine, No. 1111 Xianxia Road, Shanghai 200336, China. Email: wt.huang@hotmail.com.

Background: The liver and kidney are important metabolic organs in the body and common sites of tumor occurrence. Glycine-N-acyltransferase (GLYAT) is primarily expressed in the liver and kidney and downregulated in several tumors. But its specific functions and molecular mechanisms in liver cancer and clear cell renal cell carcinoma (ccRCC) have not yet been fully elucidated. The aim of this study was to explore the role and clinical significance of GLYAT in liver cancer and ccRCC.

Methods: This study used proteomics technology to identify differentially expressed proteins in liver cancer. Western blot and immunohistochemistry (IHC) were used to analyze the protein expression pattern of GLYAT. assays were performed in liver cancer and ccRCC cells. Xenograft models in nude mice were used to confirm the roles of GLYAT in liver cancer. Moreover, the downstream regulatory proteins of GLYAT were identified by proteomics.

Results: GLYAT was lowly expressed in liver cancer and ccRCC. Immunofluorescence staining indicated that GLYAT was mainly expressed in the cytoplasm, particularly the mitochondria. Kaplan-Meier curves showed that the low protein expression of GLYAT was correlated with a poor prognosis in liver cancer and ccRCC patients. Moreover, GLYAT expression was associated with several clinical parameters in liver cancer. Cell experiments showed that the overexpression of GLYAT inhibited cell proliferation and migration abilities; however, interfering GLYAT protein expression rescued these abilities in GLYAT overexpression (GLYAT-OE) cells. *In vivo* assays confirmed the tumor-suppressor function of GLYAT in liver cancer. Moreover, our research showed that GLYAT downregulated Rho-associated coiled-coil-containing protein kinase 1 (ROCK1).

Conclusions: Our study showed that GLYAT is lowly expressed in liver cancer and ccRCC, emphasizing its prognostic significance. It also showed that GLYAT inhibits the progression of liver cancer and ccRCC by downregulating ROCK1.

Keywords: Liver cancer; clear cell renal cell carcinoma (ccRCC); glycine-N-acyltransferase (GLYAT); prognostic markers; Rho-associated coiled-coil-containing protein kinase 1 (ROCK1)

Submitted Jul 12, 2024. Accepted for publication Aug 14, 2024. Published online Sep 27, 2024.
doi: 10.21037/tcr-24-1412
View this article at: https://dx.doi.org/10.21037/tcr-24-1412

^ ORCID: 0000-0001-8961-4196.

Introduction

Cancer is one of the leading causes of mortality, and among cancers, liver cancer is the sixth most common cancer worldwide (1). The risk factors for liver cancer mainly include virus infection (hepatitis B or C virus infection) and alcohol abuse (2). Liver cirrhosis and dysplastic nodules are important precancerous lesions of liver cancer. Renal carcinoma, which is another prevalent malignant tumor, is among the top 10 cancers in males, and leads to numerous deaths annually (1,3). Approximately 90% of renal tumor cases are attributed to renal cell carcinoma, among which clear cell renal cell carcinoma (ccRCC) accounts for around 75% of cases (4). Currently, patients with advanced liver cancer and ccRCC have a poor prognosis. Targeted therapy and immunotherapy do not greatly extend the median overall survival (OS) of advanced cancer patients (5). Thus, differential expression proteins and novel biomarkers for investigating the molecular mechanisms of tumor progression urgently need to be screened and identified.

Glycine-N-acyltransferase (GLYAT) is a member of the GCN5-related N-acetyltransferases (GNAT) superfamily and responsible for the glycine conjugation of several toxic xenobiotics, primarily the glycine conjugation of benzoic acid (6-8). The glycine conjugation of benzoic acid occurs in two steps (9). In the first step, the key enzymes are specifically expressed in the liver and kidney and are responsible for transforming benzoic acid to benzoyl-coenzyme A (CoA). In the second step, GLYAT is also specifically expressed in the liver and kidney and is responsible for conjugating benzoyl-CoA to glycine (10,11). A previous study showed that glycine conjugation rate was reduced in liver dysfunction patients (12). The variation of glycine conjugation and activity of GLYAT has also been reported to affect mitochondrial adenosine 5'-triphosphate (ATP) production, glycine availability, and CoA-SH availability (9). Thus, GLYAT is an important metabolic enzyme. GLYAT has been reported to be downregulated in liver cancer and ccRCC (11,13). Therefore, we conjectured that GLYAT plays an important role in the liver and kidney. As reported, the downregulation of GLYAT promotes breast cancer progression by regulating the PI3K/AKT/Snail signaling pathway (14). However, the functions and molecular mechanisms of GLYAT in liver cancer and ccRCC have yet to be explored.

In this study, we aimed to explore the role of GLYAT in liver cancer and ccRCC. We examined the protein expression pattern and prognostic value of GLYAT in liver cancer and ccRCC. We first explored GLYAT function *in vitro* and *in vivo* assays. We then explored the downstream regulatory proteins of GLYAT by proteomics. We supposed that GLYAT had an important tumor suppressing function in liver cancer and ccRCC. A protocol was prepared before this study, which was not registered. We present this article in accordance with the ARRIVE and MDAR reporting checklists (available at https://tcr.amegroups.com/article/view/10.21037/tcr-24-1412/rc).

Highlight box

Key findings

- Glycine-N-acyltransferase (GLYAT) has strong prognostic value in liver cancer and clear cell renal cell carcinoma (ccRCC).
- GLYAT has tumor-suppressor functions in liver cancer and ccRCC.
- GLYAT downregulates Rho-associated coiled-coil-containing protein kinase 1 (ROCK1) expression.

What is known. and what is new?

- This study first found that the downregulation of GLYAT expression is associated with a poor prognosis. *In vitro* and *in vivo* assays showed that GLYAT inhibits the progression of liver cancer and ccRCC. GLYAT also downregulates ROCK1 expression.
- ROCK1 is a protein kinase that is known to promote cancers.

What is the implication, and what should change now?

- GLYAT is a promising target for predicting prognosis and has tumor-suppressor functions in liver cancer and ccRCC.
- The regulatory mechanism underlying GLYAT and ROCK1 has yet to be explored.

Methods

Tissue samples and patient information

The study was conducted in accordance with the Declaration of Helsinki (as revised in 2013). The liver cancer tissues and patient information were obtained from the Eastern Hepatobiliary Surgery Hospital. The study was approved by the ethics board of the Eastern Hepatobiliary Surgery Hospital (No. EHBHKY2014-03-006). Informed consent was obtained from all the patients before surgery. Liver cirrhosis, low-grade dysplastic nodule (LGDN), and high-grade dysplastic nodule (HGDN) tissues were collected. We also obtained the tissue microarrays of ccRCC patients from Shanghai Outdo Biotech Co., Ltd. (Shanghai, China). Follow-up experiments and analysis of research were conducted in Tongren Hospital.

Cell culture

Liver cancer cell lines (SK-Hep1 and PLC/PRF/5), ccRCC cell lines (A498 and Caki-1), and the HEK-293T cell line were purchased from the Chinese Academy of Science (Shanghai, China). The cells were maintained in Dulbecco's modified Eagle medium (DMEM; C11995500BT; Gibco, Grand Island, NY, USA) supplemented with 10% fetal bovine serum (FBS; 10099141C; Gibco) and 1% penicillin/streptomycin (15070063; Gibco) at 37 ℃ in a 5% carbon dioxide incubator.

Western blot

The total protein of the tissues and cells were extracted using radio-immunoprecipitation assay buffer (P0013B; Beyotime Biotechnology, Shanghai, China). The isolated proteins were transferred onto polyvinylidene fluoride (PVDF) membrane (ISEQ00010; Millipore, Burlington, MA, USA). The antigen was blocked with 5% non-fat milk in tris-buffered saline with tween. GLYAT (825263; Zenbio, Chengdu, China) and Rho-associated coiled-coil-containing protein kinase 1 (ROCK1; A11158; ABclonal, Wuhan, China) antibodies were used to incubate the membrane at room temperature for 2 hours. Goat anti-rabbit immunoglobulin G (170-6515; Bio-Rad, Hercules, CA, USA) was used to incubate the membrane at room temperature for 1 hour.

Immunohistochemistry (IHC)

The methods used to prepare the tissue microarray sections and the methods used in the IHC analysis have been described in detail in a previous study (15). GLYAT (HPA044094; Sigma, Saint Louis, MO, USA) and ROCK1 (A11158, ABclonal) antibodies were used to incubate the tissue microarray section at 4 ℃ overnight. A color development kit (GK500710; Gene Tech, Shanghai, China) was used to detect the antigen. The H-scores of GLYAT and ROCK1 in each sample were calculated by HALO Multiplex IHC (version 2.3.4). The optimum cut-off values of the H-scores were calculated by the X-Tile statistical package and used to allocate the liver cancer patients (cut-off H-score: 82.84) and ccRCC patients (cut-off H-score: 95.94) to the GLYAT low expression group and the GLYAT high expression group (16).

Immunofluorescent staining

For the GLYAT stanning, we transfected the GLYAT-FLAG plasmid into PLC/PRF/5. We then seeded the cells on coverslips and used Mito-Tracker Red CMXRos (C1049B; Beyotime Biotechnology) to locate the mitochondria. The cells were fixed by 4% paraformaldehyde for 20 minutes and treated with 0.1% Triton X-100 for 5 minutes. We then used 5% FBS in phosphate-buffered saline to block the antigens. Anti-DDDDK tag primary antibody (ab250606; Abcam, Waltham, MA, USA) was incubated to bind the FLAG-tag at room temperature for 2 hours. Alexa Fluor®488-conjugated secondary antibody (SA00013-2; Proteintech, Wuhan, China) was used to incubate the cells at room temperature for 1 hour in darkness. Images were captured with a fluorescence microscope (TS2-FL; Nikon, Tokyo, Japan).

Overexpressing and interfering with GLYAT

To construct the GLYAT overexpression (GLYAT-OE) vector, we inserted the GLYAT gene full-length sequence into the pLVX-puro plasmid between the Apa I and Xba I sites. To generate lentivirus particles, we seeded the HEK-293T cells in dishes, and co-transfected the GLYAT-OE plasmids and empty vector (EV) with psPAX2 and pMD2G, respectively. The liver cancer cells (PLC/PRF/5 and SK-Hep1) and ccRCC cells (A498 and Caki-1) were infected by lentivirus particles and cultured in DMEM supplemented with 6 μg/mL puromycin. To construct the GLYAT-FLAG plasmid, we inserted GLYAT into the pCMV-C-FLAG plasmid between the Hind III and Xba I sites. This recombinant plasmid was transient transfected into the PLC/PRF/5 for immunofluorescent staining assay. Short interfering RNAs (siRNAs) for GLYAT were synthesized by Hanbio Co., Ltd. (Shanghai, China). The siRNA sequences are detailed in Table S1. Three sequences of siRNA were mixed at 100 nM and transfected into the GLYAT-OE cells. After 48 hours, we collected the cells to detect the GLYAT interfering effect and perform the cell assays.

Wound-healing and colony-formation assays

The cells were seeded in 12-well plates and cultured overnight. When the cells formed a monolayer, we scratched a cellular wound using a pipette tip. Pictures of the cellular wound were taken at different times. The wound-healing rates were computed by ImageJ software (National Institutes of Health, Bethesda, MD, USA). Colony-formation assays were used to assess cell proliferation ability. The cells were seeded into plates and incubated for 8 days. Next, crystal violet was

used to stain the cells and 4% paraformaldehyde was used to fix the cells. The cell numbers were computed by ImageJ software.

Animal studies

The animal experiments were performed under a project license (No. A2023-056-01) granted by the Ethics Committee of Tongren Hospital, in compliance with Tongren Hospital guidelines for the care and use of animals. For the cell-derived xenograft (CDX) tumor model, we purchased 3–4-week-old male BALB/c-nude mice (strain No. D000521) from GemPharmatech Co., Ltd. (Nanjing, China). The eight mice with different markers for recognizing were randomly divided into two groups and housed in specific pathogen-free conditions. Either overexpressing GLYAT SK-Hep1 cells (the treatment group) or transfected EV cells (the control group) were injected into the mice in these two groups. The volumes of tumors were measured regularly, using the following formula: volume = (length × width^2)/2. The mice were sacrificed 57 days after injection. Patient-derived xenograft (PDX) models were established in 29 mice. Based on the GLYAT H-score, 10 mice were allocated to the GLYAT positive group and 19 mice to the GLYAT negative group by X-tile. For further information and details about the methods used in the PDX model, see our previous article (17).

Statistical analysis

SPSS 26.0 (International Business Machines Corporation, New York, NY, USA) and GraphPad Prism 8.0.2 (GraphPad Software, La Jolla, MA, USA) were used for the statistical analyses. The *t*-test was used to determine if there were any statistically significant differences between the experiment group and the control group. A P value <0.05 was considered statistically significant (*, P<0.05; **, P<0.01; ***, P<0.001; ****, P<0.0001). All the experiments were performed at least three times (technical repeats).

Results

GLYAT is downregulated in liver cancer and ccRCC

We used proteomics to detect differential expression proteins in four pairs of liver cancer and adjacent tissues. In total, 274 proteins were upregulated (fold change >1.25, P<0.05) and 350 proteins were downregulated (fold change <0.83, P<0.05; *Figure 1A*). The results of the Gene Ontology (GO) enrichment analysis demonstrated that the cellular amino acid metabolic process was the most significant term, including 54 candidate proteins (*Figure 1B,1C*). From these candidates, we identified 22 genes associated with the OS of liver cancer patients using the GEPIA database (Table S2). *GLYAT* was a candidate which played an important role in metabolism. The function and mechanism of GLYAT in liver cancer have not been reported in detail. Therefore, we finally focused on *GLYAT*. Using the TIMER 2.0 and UALCAN databases, we found that GLYAT was lowly expressed in 12 types of cancers at the messenger RNA (mRNA) level, and three types of cancer at the protein level, both of which included liver cancer, ccRCC, and breast cancer (*Figure 1D,1E*). Moreover, from the UALCAN database, GLYAT was only highly expressed in liver, kidney, and breast tissues, and it was rarely expressed in other organs and tissues (14). Previous study has examined the role of GLYAT in breast cancer (14); however, this study sought to elucidate its role in liver cancer and ccRCC.

To validate the downregulation of GLYAT, we performed western blot in 10 pairs of liver cancer tissues and five pairs of ccRCC tissues and adjacent tissues. The results showed that GLYAT was significantly decreased in all liver cancer tissues (P<0.001; *Figure 2A*) and ccRCC tissues (P<0.001; *Figure 2B*). To strengthen the conclusion, we conducted IHC in tissue microarrays of 45 pairs of liver cancer and adjacent tissues, and found that GLYAT was significantly downregulated in liver cancer tissues (P<0.001; *Figure 2C*). We also performed IHC in 30 pairs of ccRCC and adjacent tissues to detect the GLYAT protein levels. As expected, GLYAT was lowly expressed in ccRCC tissues (P<0.001; *Figure 2D*). Further, IHC staining was conducted to examine the expression of GLYAT in parenchymal hepatic cells and renal tubular epithelial cells (*Figure 2E*). To clarify the subcellular localization of GLYAT, we transfected GLYAT-FLAG plasmid into PLC/PRF/5 and performed immunofluorescent staining assays. Mitochondrial probe was used to stain mitochondrial space. We found that GLYAT was well-colocalized with the mitochondrial probe (*Figure 2F*). These results showed that GLYAT is a mitochondrially expressed protein.

The downregulation of GLYAT is associated with a poor prognosis in liver cancer and ccRCC

Using the GEPIA database, we performed a Kaplan-Meier analysis to investigate the association between *GLYAT*

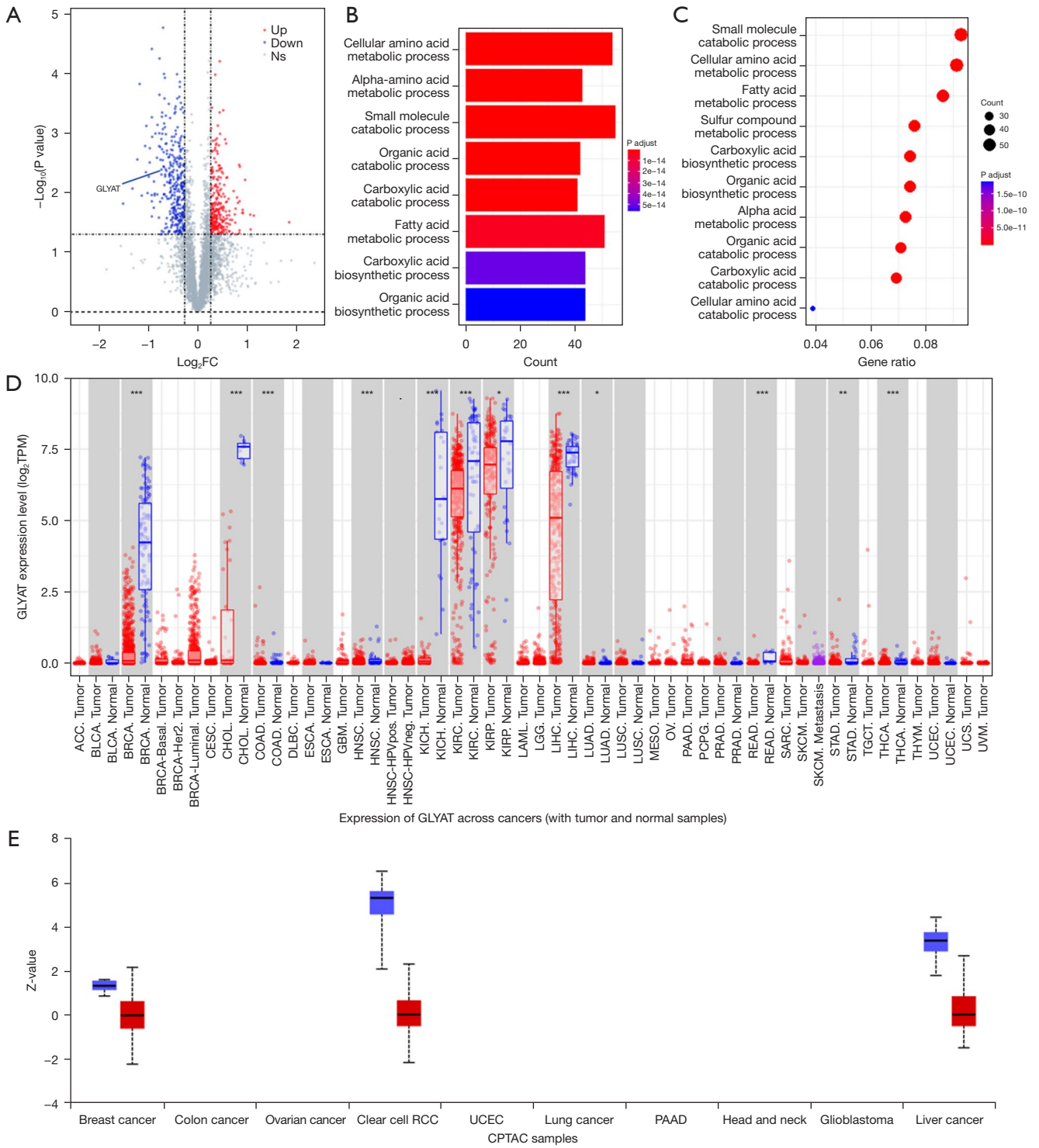

Figure 1 GLYAT is a differential expression protein in several types of cancers. (A) Differential expression proteins in liver cancer and adjacent tissues screened by proteomics. (B,C) Biological processes of the differentially expressed proteins. (D) The mRNA expression levels of GLYAT in several types of cancer samples compared with normal samples; red box represents tumor; blue box represents normal tissue; purple box represents metastatic tumor. (E) The protein expression levels of GLYAT in three types of cancer samples compared with normal samples; red box represents tumor; blue box represents normal tissue. *, P<0.05; **, P<0.01; ***, P<0.001. FC, fold change; GLYAT, glycine-N-acyltransferase; TPM, transcripts per million; RCC, renal cell carcinoma; UCEC, uterine corpus endometrial carcinoma; PAAD, pancreatic adenocarcinoma; CPTAC, Clinical Proteomic Tumor Analysis Consortium; mRNA, messenger RNA.

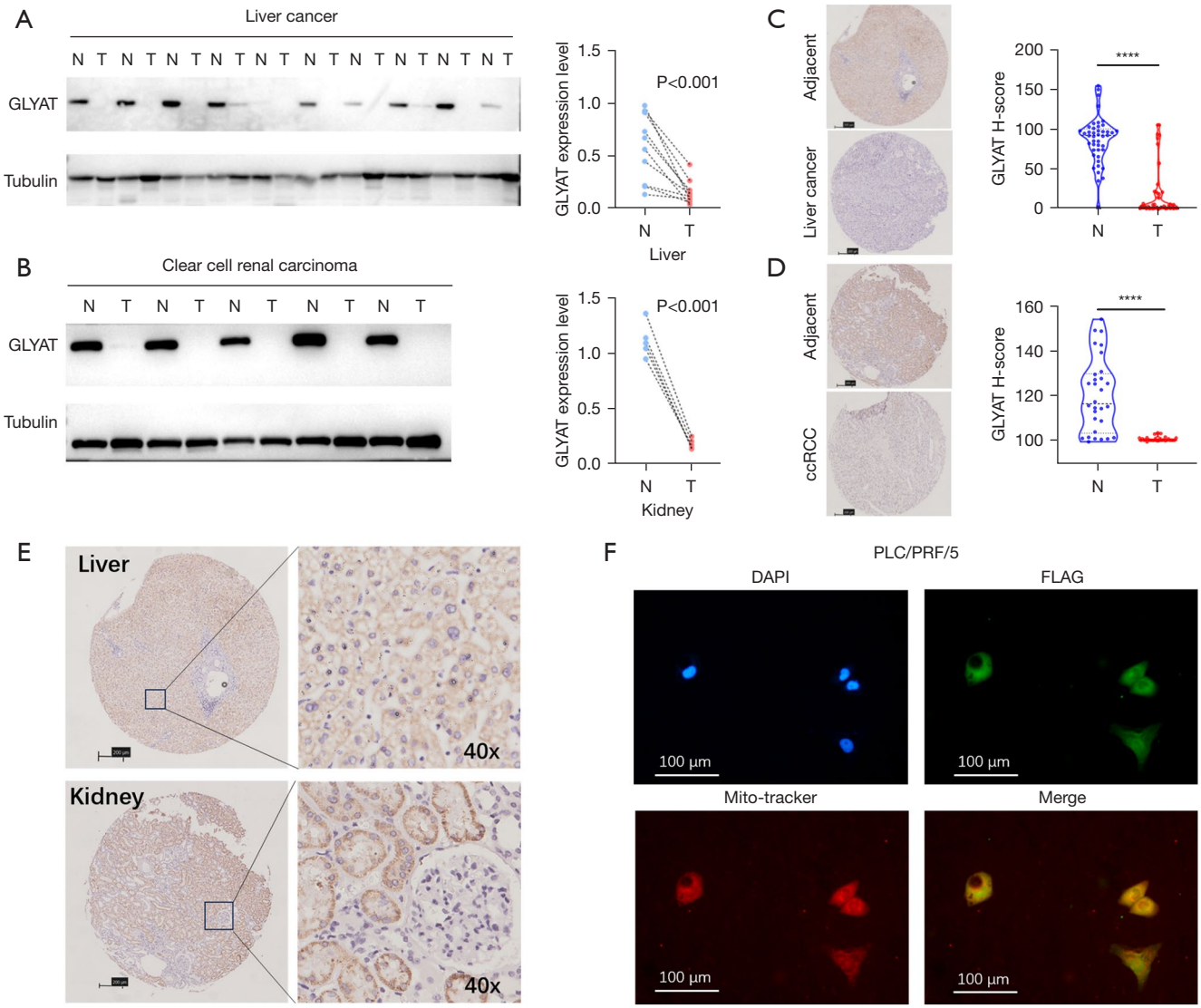

Figure 2 Expression pattern of GLYAT in liver cancer and ccRCC. (A,B) GLYAT protein expression levels in liver cancer (10 pairs) and ccRCC (5 pairs) tissues compared with adjacent tissues as detected by western blot. (C,D) GLYAT protein expression levels in liver cancer (45 pairs) and ccRCC (30 pairs) tissues compared with adjacent tissues as detected by IHC. Scale bar: 200 μm. (E) GLYAT was mainly expressed in parenchymal hepatic cells and renal tubular epithelial cells detected by IHC. Scale bar: 200 μm. (F) Immunofluorescence staining was performed in the PLC/PRF/5 cell line. FLAG: GLYAT-FLAG. Scale bar: 100 μm. ****, P<0.0001. GLYAT, glycine-N-acyltransferase; N, adjacent tissues; T, liver cancer tissues; ccRCC, clear cell renal cell carcinoma; DAPI, 4',6-diamidino-2-phenylindole; IHC, immunohistochemistry.

expression levels and the prognosis of liver cancer and ccRCC patients. The results showed that liver cancer patients with low *GLYAT* mRNA expression had a short OS (P=0.01; Figure S1A). However, there was no significant difference in the time to recurrence (TTR) between the high and low GLYAT expression cohorts (Figure S1B). In the ccRCC patients, the *GLYAT* low expression group had a short OS (P<0.001; Figure S1C) and TTR (P=0.01; Figure S1D). Overall, the downregulation of *GLYAT* may lead to a poor prognosis in liver cancer and ccRCC patients.

To validate this conclusion on protein level, we collected 288 liver cancer tissue samples and 149 RCC tissue samples

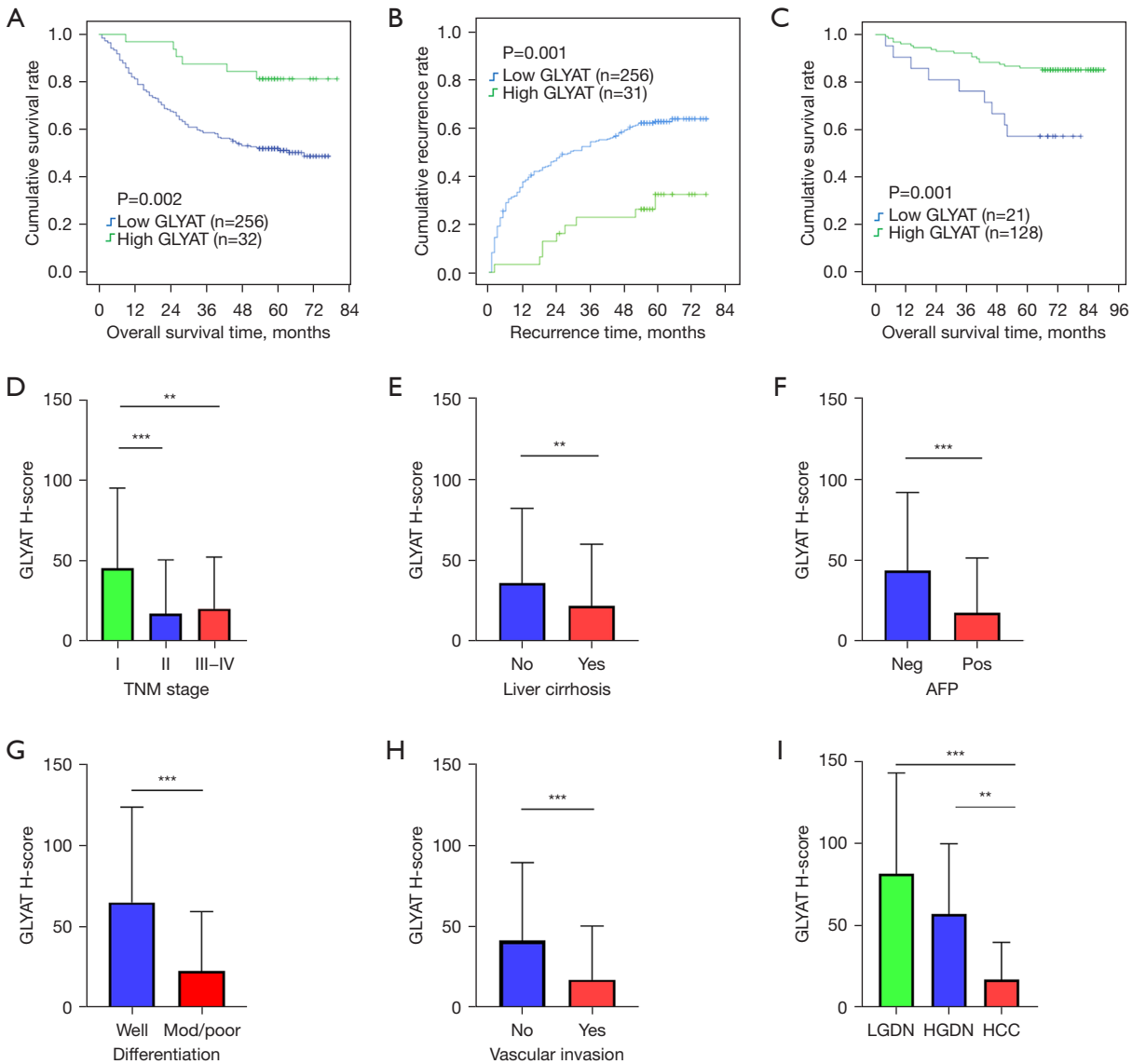

Figure 3 Prognostic values of GLYAT in liver cancer and ccRCC. (A,B) Kaplan-Meier curves for OS (n=288) and the TTR (n=287) of GLYAT in liver cancer patients. (C) Kaplan-Meier curves for OS (n=149) of GLYAT in ccRCC patients. (D-I) The relationship between GLYAT and six pathological indicators of liver cancer. **, P<0.01; ***, P<0.001. Error bars denote mean ± SD. GLYAT, glycine-N-acyltransferase; TNM, tumor-node-metastasis; AFP, alpha-fetoprotein; LGDN, low-grade dysplastic nodule; HGDN, high-grade dysplastic nodule; HCC, hepatocellular carcinoma; ccRCC, clear cell renal cell carcinoma; OS, overall survival; TTR, time to recurrence; Mod, moderate; SD, standard deviation.

with the clinical information of patients. In the liver cancer cohort, the mean OS of the patients in the GLYAT low expression group was shorter than that of the patients in the GLYAT high expression group (48.9 *vs.* 70.8 months, P=0.002; *Figure 3A*), as was the mean TTR (38.3 *vs.* 62.1 months, P=0.001; *Figure 3B*). Similarly, in the ccRCC cohort, the mean OS of the GLYAT low expression group (59.2 months) was shorter than that of the GLYAT high group (81.0 months) (P=0.001; *Figure 3C*).

To further confirm the prognostic value of GLYAT, we performed univariate and multivariate Cox regression analyses of the liver cancer patients (*Table 1*). The univariate Cox regression revealed that the GLYAT H-score and other seven factors [i.e., alpha-fetoprotein (AFP), tumor-node-metastasis (TNM) stage, liver cirrhosis, tumor size, tumor number, tumor differentiation, and vascular invasion] were

Table 1 Univariate and multivariate analysis of OS and TTR in liver cancer patients

Factors	OS (n=288)				TTR (n=287)			
	Univariate (P value)	Multivariate			Univariate (P value)	Multivariate		
		HR	95% CI	P		HR	95% CI	P
Sex: male *vs.* female	0.32				0.61			
Age (years): ≤50 *vs.* >50	0.91				0.61			
HBsAg: positive *vs.* negative	0.13				0.10			
AFP (ng/mL): ≤20 *vs.* >20	<0.001*	1.537	1.025–2.307	0.04*	0.001			
Liver cirrhosis: yes *vs.* no	0.03*	1.622	1.082–2.433	0.02*	0.001*	1.837	1.282–2.631	0.001*
TNM: I *vs.* II *vs.* III–IV	<0.001*				<0.001*			
Child-Pugh: A *vs.* B	0.11				0.15			
Tumor size (cm): ≤5 *vs.* >5	<0.001*	2.504	1.709–3.667	<0.001*	<0.001*	2.147	1.560–2.956	<0.001*
Tumor number: single *vs.* multiple	<0.001*	1.929	1.329–2.800	<0.001*	<0.001*	2.118	1.513–2.964	<0.001*
Tumor differentiation: well *vs.* moderate *vs.* poor	0.049*				0.01*			
Vascular invasion: no *vs.* yes	0.01*				0.009*			
GLYAT H-score	0.004*	0.427	0.186–0.985	0.046*	0.001*	0.427	0.216–0.844	0.01*

*, P<0.05. OS, overall survival; TTR, time to recurrence; HR, hazard ratio; CI, confidence interval; HBsAg, hepatitis B surface antigen; AFP, alpha-fetoprotein; TNM, tumor-node-metastasis; GLYAT, glycine-N-acyltransferase.

associated with OS and the TTR in liver cancer patients. The multivariate Cox regression showed that the GLYAT H-score, liver cirrhosis, tumor size, and tumor number were independent prognostic factors of OS and the TTR in liver cancer, while AFP was an independent prognostic factor of OS but not of the TTR.

The χ^2 test was used to assess the relationship between GLYAT and several clinical characteristics of the liver cancer patients. The results indicated that GLYAT protein expression level was related to AFP, TNM stage, liver cirrhosis, tumor number, tumor differentiation, and vascular invasion (*Table 2*). We also found that GLYAT was significantly downregulated in liver cancer patients with advanced stage (TNM II and TNM III–IV), liver cirrhosis, positive AFP, moderate or poor differentiation, and vascular invasion (*Figure 3D-3H*). Moreover, we collected LGDN, HGDN, and well-differentiated tissue samples from liver cancer patients, and detected the GLYAT H-scores of these precancerous lesion samples. The results showed that the GLYAT H-score of the well-differentiated liver cancer samples was significantly lower than the H-scores of the LGDN and HGDN samples (*Figure 3I*). Thus, as liver cancer progressed, the expression level of GLYAT gradually decreased. In conclusion, our results showed that GLYAT has good prognostic value and could serve as a prognostic marker in liver cancer and ccRCC.

GLYAT inhibits the migration and proliferation of liver cancer and ccRCC cells

We showed that the downregulation of GLYAT was related to poor prognosis in liver cancer and ccRCC. Subsequently, we overexpressed GLYAT in liver cancer cell lines (PLC/PRF/5 and SK-Hep1) and ccRCC cell lines (A498 and Caki-1) to investigate its role in tumor migration and proliferation (Figure S2A). The EV was used as the negative control. Furthermore, we inhibited GLYAT protein expression by GLYAT-siRNA in GLYAT-OE cells for performing rescue assays (Figure S2B,S2C). The wound-healing assay results showed that the overexpression of GLYAT significantly reduced cell migration in the SK-Hep1 and PLC/PRF/5 cell lines (*Figure 4A* and Figure S3A). Similarly, the healing rate was slower in the A498 GLYAT-OE and Caki-1 GLYAT-OE cells than the EV cells (*Figure 4B* and Figure S3B). Next, we performed colony-formation assays in these four cell lines. The results showed that the overexpression of GLYAT effectively decreased the colony number and size of the SK-Hep1 and PLC/PRF/5 cells (*Figure 4C* and Figure S3C).

Table 2 Association between clinicopathological factors and GLYAT analyzed by the χ^2 test

Variables	GLYAT H-score		χ^2	P
	Low (n=256)	High (n=32)		
Sex, n			0.321	0.77
Male	225	27		
Female	31	5		
Age (years), n			1.779	0.18
≤50	128	12		
>50	128	20		
HBsAg, n†			0.071	>0.99
Negative	35	5		
Positive	217	27		
AFP, n†			17.041	<0.001*
Negative	80	22		
Positive	173	10		
Liver cirrhosis, n			4.714	0.03*
No	79	16		
Yes	177	16		
TNM, n			33.257	<0.001*
I	70	25		
II	146	6		
III–IV	40	1		
Child-Pugh, n			3.573	0.11
A	230	32		
B	26	0		
Tumor size (cm), n			1.088	0.29
≤5	119	18		
>5	137	14		
Tumor number, n			5.486	0.01*
Single	193	30		
Multiple	63	2		
Tumor differentiation, n			35.301	<0.001*
Well	16	12		
Moderate	239	19		
Poor	1	1		
Vascular invasion, n			27.183	<0.001*
No	86	26		
Yes	170	6		

†, four cases of patients lack HBsAg information and three cases of patients lack AFP information; *, P<0.05. GLYAT, glycine-N-acyltransferase; HBsAg, hepatitis B surface antigen; AFP, alpha-fetoprotein; TNM, tumor-node-metastasis.

The same conclusion was found in relation to the A498 and Caki-1 cells (*Figure 4D* and Figure S3D). Thus, the results showed that GLYAT also inhibited the proliferation ability of the liver cancer and ccRCC cells.

Then, we confirmed the tumor-suppressor function of GLYAT by rescue assays. As expected, the wound-healing assays showed that the disruption of GLYAT in the SK-Hep1 GLYAT-OE cells and A498 GLYAT-OE cells re-enhanced the migration ability of the cells (Figure S4A,S4B). Similarly, the colony-formation assays showed that inhibited GLYAT prompted the proliferation ability of the cells (Figure S4C,S4D).

To further validate the function of GLYAT *in vivo*, a CDX model was established in the nude mice by injecting SK-Hep1 GLYAT-OE and EV cells. Tumor growth was monitored regularly. As shown in the growth curve, the tumor volumes of the GLYAT-OE group (n=4) were smaller than those of the EV group (n=4; *Figure 4E*). Additionally, we established a PDX model in nude mice. According to the GLYAT H-score, we divided the liver cancer tissues into the GLYAT positive group (n=10) and the GLYAT negative group (n=19). The results showed that the tumors derived from the GLYAT positive group were smaller than those derived from the GLYAT negative group (*Figure 4F*). These findings collectively showed that GLYAT played an important role in tumor suppression both *in vitro* and *in vivo*.

GLYAT downregulates ROCK1 expression in liver cancer and ccRCC

The above-mentioned results of our study showed that GLYAT acted as a tumor suppressor in liver cancer and ccRCC. To elucidate the underlying mechanism of the GLYAT tumor-suppressor function, we used proteomics to identify the differential expression proteins in the GLYAT overexpressed and disrupted A498 cells. The results showed that 244 proteins were upregulated and 219 proteins were downregulated in the A498 GLYAT-OE cells. Additionally, 313 proteins were downregulated and 307 proteins were upregulated in the A498 GLYAT-OE cells after they had been disturbed by GLYAT-siRNA (Figure S5A). A comparison of these groups revealed that 135 differential expression proteins overlapped (*Figure 5A*). The results of the GO analysis showed that 15 proteins were enriched in the following three terms related to the apoptotic biology process: the motor neuron apoptotic process, the negative regulation of apoptotic process, and the regulation of apoptotic process (Figure S5B). Among

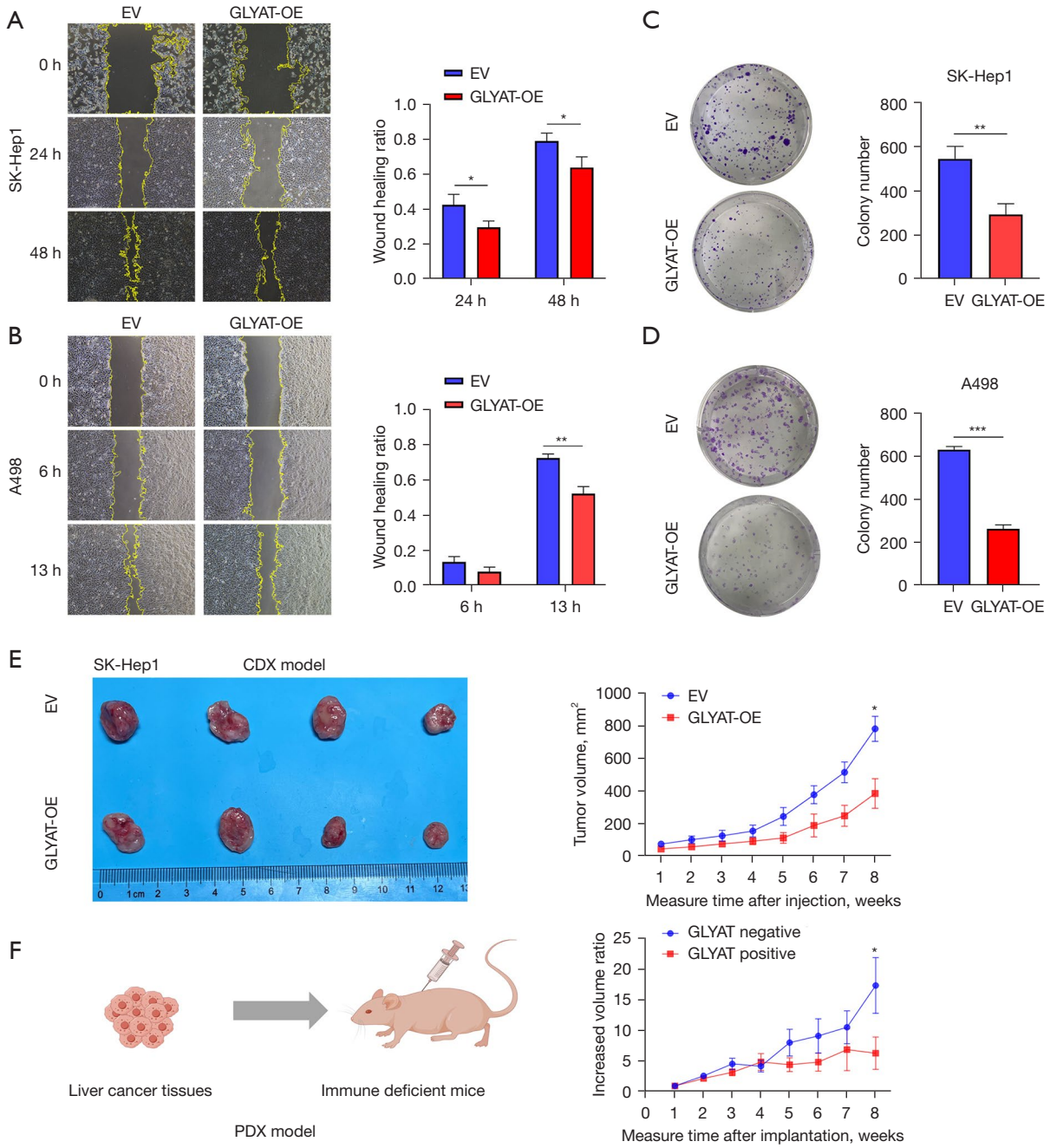

Figure 4 GLYAT suppressed tumor growth and migration *in vitro* and *in vivo*. (A,B) Wound healing assay showed that overexpressed GLYAT inhibited the migration ability of the liver cancer and ccRCC cells (40×). Error bars denote mean ± SD. (C,D) The overexpression of GLYAT inhibited the proliferation ability of the liver cancer and ccRCC cells. Cells were stained by crystal violet. Error bars denote mean ± SD. (E) The effects of GLYAT on tumor growth in the CDX models. Error bars denote mean ± SEM. (F) The effects of GLYAT on tumor growth in the PDX models. Error bars denote mean ± SEM. *, P<0.05; **, P<0.01; ***, P<0.001. EV, empty vector; GLYAT-OE, GLYAT overexpression; GLYAT, glycine-N-acyltransferase; CDX, cell-derived xenograft; PDX, patient-derived xenograft; ccRCC, clear cell renal cell carcinoma; SD, standard deviation; SEM, standard error of the mean.

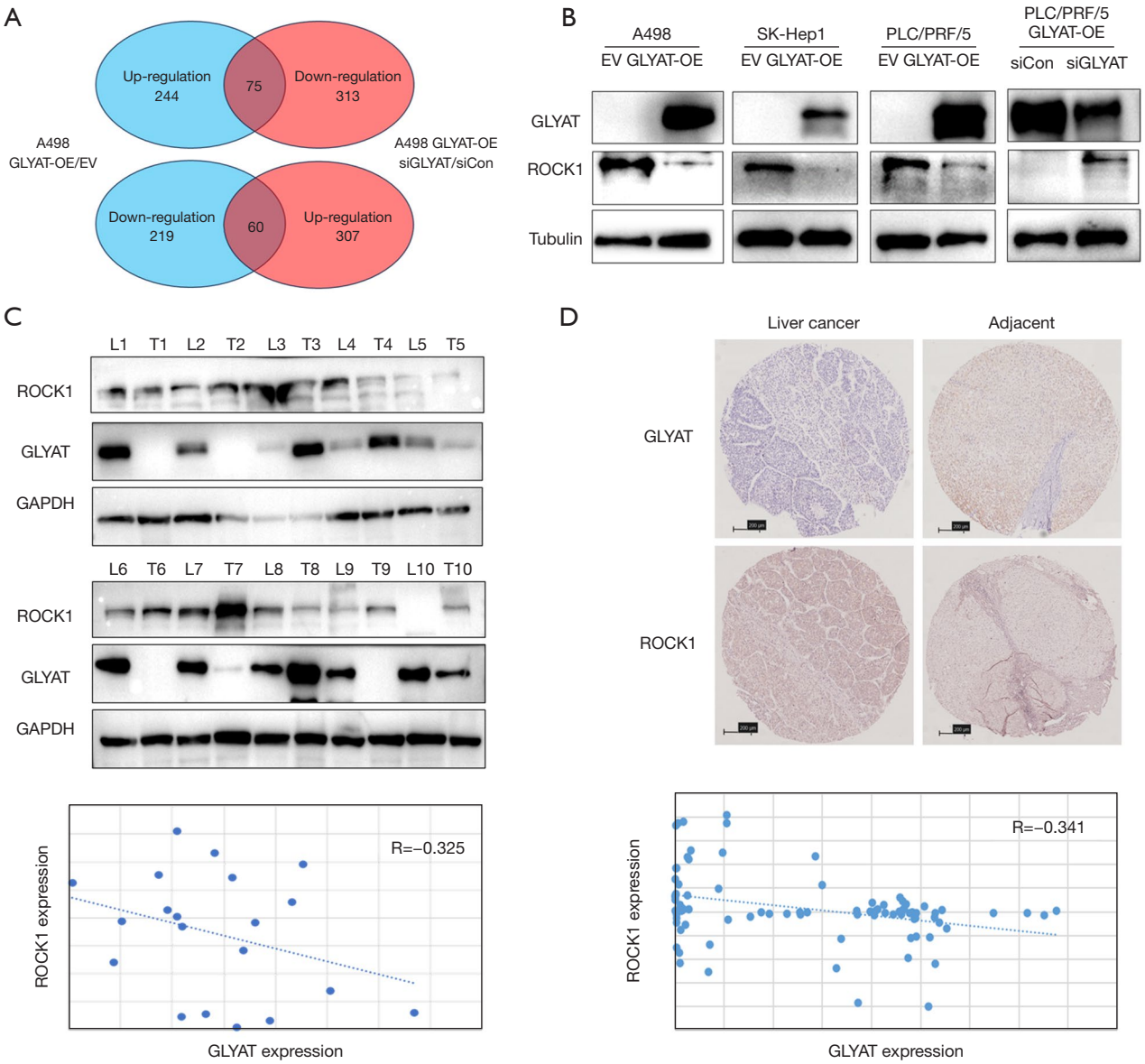

Figure 5 GLYAT suppressed tumor growth and migration *in vitro* and *in vivo*. (A) Differential expression proteins overlapped between upregulated proteins after overexpressing GLYAT and downregulated proteins after inhibiting GLYAT by siRNA, as well as downregulated proteins after overexpressing GLYAT and upregulated proteins after inhibiting GLYAT. (B) The effect of overexpressing and inhibiting GLYAT on ROCK1 protein expression. (C,D) The association between GLYAT and ROCK1 protein expression detected by western blot in 10 pairs of liver cancer and adjacent tissues and IHC in 45 pairs of liver cancer and adjacent tissues. Scale bar: 200 μm. GLYAT-OE, GLYAT overexpression; GLYAT, glycine-N-acyltransferase; EV, empty vector; si, short interfering RNA; Con, control group; ROCK1, Rho-associated coiled-coil-containing protein kinase 1; GAPDH, glyceraldehyde-3-phosphate dehydrogenase; IHC, immunohistochemistry.

these candidate proteins, ROCK1 is one of the five most significant differential proteins. The downregulation of GLYAT promotes breast cancer by the PI3K/AKT/Snail pathway (14). We focused on whether ROCK1 promotes PI3K activation (18).

To verify the association between ROCK1 and GLYAT, we performed western blot and found that ROCK1 was downregulated in the GLYAT-OE cells (A498, SK-Hep1, and PLC/PRF/5; *Figure 5B*). Conversely, ROCK1 was upregulated after GLYAT interference in the A498 GLYAT-

OE cells (*Figure 5B*). To further verify the relationship between GLYAT and ROCK1, we measured the protein expression levels of GLYAT and ROCK1 in 10 pairs of tissues by western blot. The result revealed that ROCK1 protein expression was negatively correlated with GLYAT (R=–0.325; *Figure 5C*). We confirmed this conclusion in 45 pairs of liver cancer and adjacent tissues by IHC (R=–0.341; *Figure 5D*). From the experiments above, we demonstrated that GLYAT downregulated ROCK1 protein expression.

Discussion

The development of multiple omics techniques has helped to elucidate tumor heterogeneity (19). The dysregulation of protein expression plays an important role in tumor initiation and progression (20-22). Proteomics is helpful in identify differential expression proteins, which can be used as novel tumor molecular markers for liver cancer and ccRCC (23,24). Proteomics has shown that GLYAT is a downregulated protein in liver cancer and ccRCC and is responsible for catalyzing the glycine conjugation of xenobiotics (7-9). GLYAT is predominantly expressed in the liver and kidney, which suggests that it may be associated with the metabolic process (10,11). As previously reported, GLYAT also plays a significant role in metabolism, especially in the maintenance of intracellular CoA-SH homeostasis (9). As an important cofactor, CoA-SH plays a central role in the oxidation of pyruvate in the citric acid cycle, as well as in the metabolism of carboxylic acids (including short- and long-chain fatty acids) (25-28). According to previous research, GLYAT is a renal function-related target in acute kidney injury (29). Guo *et al.* also reported that GLYAT participates in the co-regulation of bone phenotypes and body lean mass (30). Moreover, GLYAT is reported to have a tumor-suppressor function in breast cancer (14).

First, we found that GLYAT was lowly expressed in liver cancer and ccRCC by western blot and IHC. The IHC results showed that GLYAT was mainly expressed in liver parenchyma and renal tubular cells. The immunofluorescence results further showed that GLYAT was mainly located in the mitochondria of liver cancer cells, which is consistent with previous research (11). However, the subcellular localization of GLYAT in ccRCC cells required verification. Thus, we analyzed the prognostic value of GLYAT in liver cancer and ccRCC patients. The Kaplan-Meier analysis showed that the liver cancer and ccRCC patients with low GLYAT expression had shorter OS than those with high GLYAT expression. The TTR of liver cancer patients with low GLYAT expression was also shorter than that of patients with high GLYAT expression. Moreover, the univariate and multivariate Cox regression analyses showed that GLYAT was an independent prognostic factor for liver cancer. We also found that the expression level of the GLYAT protein was correlated with TNM stage, liver cirrhosis, AFP, tumor differentiation, and vascular invasion.

As far as we know, this is the first study to validate the prognostic value of GLYAT protein expression in liver cancer and ccRCC. Previous research has reported that the development of liver cancer usually follows a multistep process: liver cirrhosis transform into dysplastic nodules (LGDNs and HGDNs), which then transform into liver cancer (31). Among which, the formation of HGDNs is the last step before transformation to liver cancer (32,33). The occurrence of liver cancer has previously been reported to be accompanied by alterations in the protein expression profile (34). To further explore the alteration of GLYAT protein expression in the progress of liver cancer occurrence, we also collected tissue samples of LGDNs, HGDNs, and well-differentiated liver cancer. We discovered that the expression level of GLYAT was still high in the LGDNs, while the expression level of GLYAT protein was the lowest in the liver cancer tissues. This indicates that the protein expression level of GLYAT protein gradually decreases during the development of liver cancer. The downregulation of GLYAT might play a key role in the occurrence and malignant progression of liver cancer.

To investigate the tumor-suppressor function of GLYAT in liver cancer and ccRCC, we performed cell and animal experiments. The wound-healing and colony-formation assays illustrated that GLYAT significantly inhibited cell proliferation and migration. Meanwhile, disturbing GLYAT protein expression rescued cell proliferation and migration. The CDX tumor model results also verified that the overexpression of GLYAT inhibited tumor growth in nude mice. Nude mice represent an important experimental model for cancer research (35). We also established PDX tumor model that could more realistically represent tumor heterogeneity and genetic characteristics (36). Not surprisingly, the PDX tumor model further confirmed the suppressor role of GLYAT.

Further, we showed that GLYAT downregulated ROCK1 expression. We also found that the ROCK1 expression levels were associated with the GLYAT expression levels in the liver cancer and adjacent tissues. ROCK1 is a serine/threonine protein kinase that is involved in the regulation

of cell morphology, the regulation of gene expression, cell proliferation and differentiation, the apoptotic process, and the carcinogenic process (37). Currently, tyrosine kinase inhibitors are still important treatment of liver cancer (38). As a serine/threonine kinase, ROCK1 may provide personalized guidance and serve as a potential target for liver cancer patients. ROCK1 has also been reported to be involved in the malignant progression of common tumors, such as ovarian cancer, bladder cancer, and colon cancer (39-41). As we known, ROCK1 was a downstream protein in tyrosine kinase Met (c-Met) pathway and participate in malignant tumor progression together with c-Met (41). Santoro *et al.* reported that MET inhibitor was effective in the treatment of liver cancer (42). Therefore, we speculate that GLYAT and ROCK1 may have potential to be used as therapeutic targets. Hu *et al.* showed that RCOK1 promotes the invasion and migration of non-small cell lung cancer by phosphorylating the PTEN/PI3K/FAK pathway (18). We conjecture that the downregulation of GLYAT might promote tumor progression by phosphorylating PI3K and downstream proteins by elevating ROCK1 protein expression. The knockdown of ROCK1 protein expression or the inhibition of ROCK1 protein activity has been shown to effectively inhibit the growth of liver cancer and renal cancer cells (43,44). Therefore, we suggest that GLYAT may act as a tumor suppressor in liver cancer and ccRCC by inhibiting ROCK1 expression. However, the regulatory mechanism between GLYAT and ROCK1 has yet to be explored.

Conclusions

In conclusion, GLYAT exhibits low protein expression levels in liver cancer and ccRCC. Our results indicate that the decreased expression of GLYAT protein is associated with a poor prognosis in patients with these cancers, which suggests that it could serve as a prognostic molecular marker. Both the *in vitro* and *in vivo* assays showed the inhibitory effects of GLYAT on liver cancer and ccRCC cells. Further, we also discovered that GLYAT may exert its anti-tumor effect by downregulating ROCK1 expression. Overall, our study highlights the significance of GLYAT in liver cancer and ccRCC.

Acknowledgments

We would like to thank Tongren Hospital for supporting this study. We would like to thank Wen-Ming Cong (Eastern Hepatobiliary Surgery Hospital, Shanghai, China) and Ju-Tang Li (Tongren Hospital, Shanghai, China) for help in our research. We also thank Dr. Łukasz Zapała (Clinic of General, Oncological and Functional Urology, Medical University of Warsaw, Warsaw, Poland) for the critical comments and valuable advice on this study.

Funding: This work was supported by the National Nature Science Foundation of China (No. 81972574), the Leading Talents of Tongren Hospital Fund (No. TRKYRC-lj202205), and the Medical-Engineering Combination Fund (No. 2023DHYGJC-ZDB01).

Footnote

Reporting Checklist: The authors have completed the ARRIVE and MDAR reporting checklists. Available at https://tcr.amegroups.com/article/view/10.21037/tcr-24-1412/rc

Data Sharing Statement: Available at https://tcr.amegroups.com/article/view/10.21037/tcr-24-1412/dss

Peer Review File: Available at https://tcr.amegroups.com/article/view/10.21037/tcr-24-1412/prf

Conflicts of Interest: All authors have completed the ICMJE uniform disclosure form (available at https://tcr.amegroups.com/article/view/10.21037/tcr-24-1412/coif). The authors have no conflicts of interest to declare.

Ethical Statement: The authors are accountable for all aspects of the work in ensuring that questions related to the accuracy or integrity of any part of the work are appropriately investigated and resolved. The study was conducted in accordance with the Declaration of Helsinki (as revised in 2013). The study was approved by the ethics board of the Eastern Hepatobiliary Surgery Hospital (No. EHBHKY2014-03-006) and informed consent was taken from all the patients. Animal experiments were performed under a project license (No. A2023-056-01) granted by the Ethics Committee of Tongren Hospital, in compliance with Tongren Hospital guidelines for the care and use of animals.

References

1. Sung H, Ferlay J, Siegel RL, et al. Global Cancer Statistics 2020: GLOBOCAN Estimates of Incidence and Mortality Worldwide for 36 Cancers in 185 Countries. CA Cancer J Clin 2021;71:209-49.
2. Global Burden of Disease Liver Cancer Collaboration; Akinyemiju T, Abera S, et al. The Burden of Primary Liver Cancer and Underlying Etiologies From 1990 to 2015 at the Global, Regional, and National Level: Results From the Global Burden of Disease Study 2015. JAMA Oncol 2017;3:1683-91.
3. Siegel RL, Miller KD, Fuchs HE, et al. Cancer Statistics, 2021. CA Cancer J Clin 2021;71:7-33.
4. Hsieh JJ, Purdue MP, Signoretti S, et al. Renal cell carcinoma. Nat Rev Dis Primers 2017;3:17009.
5. Ladd AD, Duarte S, Sahin I, et al. Mechanisms of drug resistance in HCC. Hepatology 2024;79:926-40.
6. Neuwald AF, Landsman D. GCN5-related histone N-acetyltransferases belong to a diverse superfamily that includes the yeast SPT10 protein. Trends Biochem Sci 1997;22:154-5.
7. Kühn S, Williams ME, Dercksen M, et al. The glycine N-acyltransferases, GLYAT and GLYATL1, contribute to the detoxification of isovaleryl-CoA - an in-silico and in vitro validation. Comput Struct Biotechnol J 2023;21:1236-48.
8. van der Sluis R, Badenhorst CP, Erasmus E, et al. Conservation of the coding regions of the glycine N-acyltransferase gene further suggests that glycine conjugation is an essential detoxification pathway. Gene 2015;571:126-34.
9. Badenhorst CP, van der Sluis R, Erasmus E, et al. Glycine conjugation: importance in metabolism, the role of glycine N-acyltransferase, and factors that influence interindividual variation. Expert Opin Drug Metab Toxicol 2013;9:1139-53.
10. Fagerberg L, Hallström BM, Oksvold P, et al. Analysis of the human tissue-specific expression by genome-wide integration of transcriptomics and antibody-based proteomics. Mol Cell Proteomics 2014;13:397-406.
11. Matsuo M, Terai K, Kameda N, et al. Designation of enzyme activity of glycine-N-acyltransferase family genes and depression of glycine-N-acyltransferase in human hepatocellular carcinoma. Biochem Biophys Res Commun 2012;420:901-6.
12. Furuya KN, Durie PR, Roberts EA, et al. Glycine conjugation of para-aminobenzoic acid (PABA): a quantitative test of liver function. Clin Biochem 1995;28:531-40.
13. Muñoz JP, Calaf GM. Downregulation of Glycine N-Acyltransferase in Kidney Renal Clear Cell Carcinoma: A Bioinformatic-Based Screening. Diagnostics (Basel) 2023;13:3505.
14. Tian X, Wu L, Jiang M, et al. Downregulation of GLYAT Facilitates Tumor Growth and Metastasis and Poor Clinical Outcomes Through the PI3K/AKT/Snail Pathway in Human Breast Cancer. Front Oncol 2021;11:641399.
15. Wang J, Xia YC, Tian BX, et al. Novel quantitative immunohistochemistry method using histone H3, family 3B as the internal reference standard for measuring human epidermal growth factor receptor 2 expression in breast cancer. Cancer 2024;130:1424-34.
16. Camp RL, Dolled-Filhart M, Rimm DL. X-tile: a new bio-informatics tool for biomarker assessment and outcome-based cut-point optimization. Clin Cancer Res 2004;10:7252-9.
17. Yu H, Mei XP, Su PF, et al. A poor prognosis in human hepatocellular carcinoma is associated with low expression of DPP4. Braz J Med Biol Res 2020;53:e9114.
18. Hu C, Zhou H, Liu Y, et al. ROCK1 promotes migration and invasion of non-small-cell lung cancer cells through the PTEN/PI3K/FAK pathway. Int J Oncol 2019;55:833-44.
19. Li Y, Lih TM, Dhanasekaran SM, et al. Histopathologic and proteogenomic heterogeneity reveals features of clear cell renal cell carcinoma aggressiveness. Cancer Cell 2023;41:139-163.e17.
20. Mustafa GM, Larry D, Petersen JR, et al. Targeted proteomics for biomarker discovery and validation of hepatocellular carcinoma in hepatitis C infected patients. World J Hepatol 2015;7:1312-24.
21. Jiang Y, Sun A, Zhao Y, et al. Proteomics identifies new therapeutic targets of early-stage hepatocellular carcinoma. Nature 2019;567:257-61.
22. Clark DJ, Dhanasekaran SM, Petralia F, et al. Integrated Proteogenomic Characterization of Clear Cell Renal Cell Carcinoma. Cell 2019;179:964-983.e31.
23. Hong S, Zhang J, Liu S, et al. Protein profiles reveal MSH6/MSH2 as a potential biomarker for hepatocellular carcinoma with microvascular invasion. Hepatol Res 2024;54:189-200.

24. Park J, Lee EH, Sim H, et al. Using Comparative Proteomics to Identify Protein Signatures in Clear Cell Renal Cell Carcinoma. Cancer Genomics Proteomics 2023;20:592-601.
25. Fromenty B, Pessayre D. Inhibition of mitochondrial beta-oxidation as a mechanism of hepatotoxicity. Pharmacol Ther 1995;67:101-54.
26. Zhang YM, Chohnan S, Virga KG, et al. Chemical knockout of pantothenate kinase reveals the metabolic and genetic program responsible for hepatic coenzyme A homeostasis. Chem Biol 2007;14:291-302.
27. Wanders RJ, Vreken P, den Boer ME, et al. Disorders of mitochondrial fatty acyl-CoA beta-oxidation. J Inherit Metab Dis 1999;22:442-87.
28. Eaton S, Bartlett K, Pourfarzam M. Mammalian mitochondrial beta-oxidation. Biochem J 1996;320 (Pt 2):345-57.
29. Zhang Y, Cai J, Lu W, et al. Comprehensive Network-Based Analyses Reveal Novel Renal Function-Related Targets in Acute Kidney Injury. Front Genet 2022;13:907145.
30. Guo YF, Zhang LS, Liu YJ, et al. Suggestion of GLYAT gene underlying variation of bone size and body lean mass as revealed by a bivariate genome-wide association study. Hum Genet 2013;132:189-99.
31. Jee BA, Choi JH, Rhee H, et al. Dynamics of Genomic, Epigenomic, and Transcriptomic Aberrations during Stepwise Hepatocarcinogenesis. Cancer Res 2019;79:5500-12.
32. Iavarone M, Manini MA, Sangiovanni A, et al. Contrast-enhanced computed tomography and ultrasound-guided liver biopsy to diagnose dysplastic liver nodules in cirrhosis. Dig Liver Dis 2013;45:43-9.
33. Di Tommaso L, Sangiovanni A, Borzio M, et al. Advanced precancerous lesions in the liver. Best Pract Res Clin Gastroenterol 2013;27:269-84.
34. Zhu H, Lin Y, Lu D, et al. Proteomics of adjacent-to-tumor samples uncovers clinically relevant biological events in hepatocellular carcinoma. Natl Sci Rev 2023;10:nwad167.
35. Szadvari I, Krizanova O, Babula P. Athymic nude mice as an experimental model for cancer treatment. Physiol Res 2016;65:S441-53.
36. Abdolahi S, Ghazvinian Z, Muhammadnejad S, et al. Patient-derived xenograft (PDX) models, applications and challenges in cancer research. J Transl Med 2022;20:206.
37. Rath N, Olson MF. Rho-associated kinases in tumorigenesis: re-considering ROCK inhibition for cancer therapy. EMBO Rep 2012;13:900-8.
38. Llovet JM, Kelley RK, Villanueva A, et al. Hepatocellular carcinoma. Nat Rev Dis Primers 2021;7:6.
39. Pan L, Meng Q, Li H, et al. LINC00339 promotes cell proliferation, migration, and invasion of ovarian cancer cells via miR-148a-3p/ROCK1 axes. Biomed Pharmacother 2019;120:109423.
40. Dai R, Zhou Y, Chen Z, et al. Lnc-MUC20-9 binds to ROCK1 and functions as a tumor suppressor in bladder cancer. J Cell Biochem 2020;121:4214-25.
41. Tsai HL, Tsai YC, Chen YC, et al. MicroRNA-148a induces apoptosis and prevents angiogenesis with bevacizumab in colon cancer through direct inhibition of ROCK1/c-Met via HIF-1α under hypoxia. Aging (Albany NY) 2022;14:6668-88.
42. Santoro A, Simonelli M, Rodriguez-Lope C, et al. A Phase-1b study of tivantinib (ARQ 197) in adult patients with hepatocellular carcinoma and cirrhosis. Br J Cancer 2013;108:21-4.
43. Wu H, Chen Y, Li B, et al. Targeting ROCK1/2 blocks cell division and induces mitotic catastrophe in hepatocellular carcinoma. Biochem Pharmacol 2021;184:114353.
44. Qin Z, Wei X, Jin N, et al. MiR-199a targeting ROCK1 to affect kidney cell proliferation, invasion and apoptosis. Artif Cells Nanomed Biotechnol 2018;46:1920-5.

Cite this article as: Xia Y, Huang W, Jin GZ. GLYAT suppresses liver cancer and clear cell renal cell carcinoma progression by downregulating ROCK1 expression. Transl Cancer Res 2024;13(9):5097-5111. doi: 10.21037/tcr-24-1412